Assessment of drought stress in arid olive groves using HidroMORE model

Abderrahman Sghaier, Hanen Dhaou, Lassaad Jarray, Zouhair Abaab, Ahmed Sekrafi, Mohamed Ouessar

Laboratory of Eremology and Combating Desertification, Institute for Arid Regions, University of Gabes, Médenine, Tunisia

Abstract

The olive tree is well known for being adapted to the arid conditions of the Mediterranean basin. However, prolonged drought periods which are expected to become more frequent because of climate change could result in severe water stress. In order to map the spatial distribution of drought stress in the olive groves in the arid regions of southeastern Tunisia (governorate of Médenine), we made recourse to the HidroMORE model (based mainly on FAO56 ET, NDVI from Sentinel 2 images and other physical parameters) to compute the water balance in a GIS environment. The outputs were compared to in situ soil water content measurements in four selected sites representing the various agro-ecological zones (mountains, piedmont, inner plain and coast) of the study site during the observation period from January 2016 to December 2019. The model outputs performed relatively well (the overall correlation coefficient R^2=0.72; index of agreement IA=0.76). The simulation results show that during normal years or average droughts, the water stress is least in the mountain and piedmont zones because of the additional runoff water supplied by the traditional water harvesting structures (*Jessour* and *Tabias*) and in the coastal zone, thanks to the higher air humidity and rainfall. In contrast, the olives in the inner plains are the most affected. Nevertheless, in case of severe droughts, the stress is generalised. Thus, the model could be used as a decision tool for prioritizing areas of intervention for drought control and mitigation (supplemental irrigation for trees safeguard, *etc*.)

Correspondence: Abderrahman Sghaier, Laboratory of Eremology and Combating Desertification (LR16IRA01), Institute for Arid Regions (Institut des Régions Arides, IRA), University of Gabes, Médenine, Tunisia.
E-mail: abderrahman.sghaier@gmail.com

Key words: Olive; arid; soil water balance; HidroMORE model; drought; geomatics.

Acknowledegements: this work was carried out as part of the ERANETMED3-068 OptiMED-Water Project funded by the EU. It was also undertaken in the framework of the research programs of the Laboratory of Eremology and Combating Desertification of IRA (LR16IRA01) funded by the Tunisian Ministry of Higher Education and Scientific Research.

Received for publication: 24 August 2021.
Accepted for publication: 19 December 2021.

Journal of Agricultural Engineering 2022; LIII:1264
doi:10.4081/jae.2022.1264

Introduction

Largely believed to be originated in the Mediterranean basin, the olive tree (*Olea europaea L.*) has been cultivated for more than 6500 years. Nowadays, it represents one of the most strategic sectors in the agricultural production system of the European Union and Tunisia, being respectively the first and the second producer of olive oil in the world (Langgut *et al*., 2019; Fraga *et al*., 2021). Moreover, the sector is experiencing a rapid increase in the number of plantations influenced by the constantly growing demand for the main products (olive oil and table olives) (Fernández-Uclés *et al*., 2020). Throughout centuries, farmers have overcome numerous obstacles and adapted to various changes. However, in recent years the cultivation of this species has been facing a new set of challenges related to climate changes. Those challenges are unprecedented and are coming at a high pace, making adapting to them more demanding and problematic (Estrada *et al*., 2020). Increase in temperature, decrease in precipitation, change in rainfall patterns, and more frequent extreme weather events such as prolonged episodes of drought and heatwaves are some of the expected changes (Vogel *et al*., 2021; Yves *et al*., 2020; Mimeau *et al*., 2021). Olive orchards do not only play an essential economic role, *i.e*., they are a major source of income for rural households, in fact; i) they also play a social role as they slow the rate of urban migration and offer work opportunities for the marginal areas (Fraga *et al*., 2021; Nasr *et al*., 2021) and ii) an environmental role since by combating desertification and erosion via the installation of traditional water harvesting techniques (namely Jessour and Tabia) they limit the effect of wind and water erosion (Soula *et al.*, 2021). Remote sensing data have been extensively used to estimate plant evapotranspiration (Zhang *et al.*, 2016). This approach is advantageous because it allows the monitoring of the tree growth and annual cycle (Spyropoulos *et al*., 2020) besides offering data on the current state of the orchard (Khanal *et al*., 2020). However, assessing olive orchard evapotranspiration is particularly difficult for several reasons: first, it is common for olive orchards to be located on steep hilly slopes (Schiettecatte *et al*., 2005) where various types of soil conservation and/or water harvesting techniques are installed. Those structures are capable of increasing the amount of available soil water for the trees, which can make the difference in the survival of the trees, particularly in arid environments (Ouessar *et al*., 2008, 2009; Ouessar, 2017). Second, different cropping systems are used in olive orchards: the traditional and the intense (Sbitri and Serafini, 2007). From a crop management standpoint, those systems differ as much as an entirely different crop species (Fernández-Escobar

et al., 2013). Third, the domesticated olive tree (*olea europaea*) is unique among all fruit-bearing tree species because it is the only one domesticated separately on several occasions throughout human history (Besnard and Bervillé, 2000). Therefore, olive possesses a great genetic variability, which makes studying olive-tree behaviour a challenging task. Because it affects several key phenotypical features of the tree, such as the tree vigour, resilience to drought, yield productivity, and adaptability to poor soils. Furthermore, the olive-tree management practices vary significantly across the regions and the available resources, affecting all the tree management components namely: soil management, irrigation (including rainfed), fertilization, pruning, and fruit harvesting (Vossen, 2007; Fernández-Escobar *et al*., 2013). Consequently, special attention must be given to the model parametrisation and model input. It is possible to estimate the evapotranspiration, either by using the surface energy balance (SEB) approach or the soil water balance (SWB). The former relies on the surface temperature provided by the satellite data as a primary input to estimate the surface latent heat flux (Wagle *et al*., 2017; Senkondo *et al*., 2019; Ortega-Salazar *et al*., 2021), and the latter is based on the spectral vegetation indices (Santos, 2018; Huang *et al*., 2021). These indices are particularly useful in conveying an accurate assessment of the plant's potential transpiration under water stress conditions (Ferreira, 2017; Zhang *et al*., 2017). Throughout the last few decades, the scientific community has been well-aware of the specificity of the olive-tree water balance. This led to the development of a plethora of models to address this issue. Some are generic, whereas others are specifically tailored for olive trees. WABOL and the model developed by Moriondo *et al*. (2019) are process-based models specific to olive trees relying on a relatively small set of inputs and providing robust results (Abazi *et al*., 2013; Gómez *et al*., 2014; Piras *et al*., 2021). However, they are not spatially distributed, and they cannot take remote sensing data as inputs. Other models such as AquaCrop and SWAT, which are based on the water availability as the limiting factor, are effective and have been used successfully to model water balance in many olive cropping systems (Ouessar *et al*., 2009; Raes *et al*., 2009; Napoli and Orlandini, 2015). However, they rely on the assumption that the ground cover is homogeneous. This can significantly affect their performances in sparse plantations conditions, characterizing the traditional olive tree orchards in arid environments.

On the other hand, models such as SVAT, SAMIR and SPARSE are based on the surface energy approach, which can use the remotely sensed data (Cammalleri *et al*., 2010; Saadi *et al*., 2015, 2018). This is of great use for the sparse, vast, and hard-to-access olive orchards. Additionally, it is easier to separate evaporation from transpiration when this method is used. Nevertheless, parametrizing models that use this approach is more complicated. Also, parametrization of such models is often zone limited thus it may be a hurdle when applying the model to extensive olive groves. Therefore, we have a gap in models that can use remote sensing data on large heterogenous areas to produce results in a simple spatial format that can be read and interpreted easily by farmers. The main objective of this study is to develop a decision support system able to exploit remote sensing data combined with field measurements for the spatial assessment of drought-affected olive groves in the arid areas of southern Tunisia. This system can help identify vulnerable areas and optimize mitigation interventions.

Materials and methods

Study area description

The study area covers entirely the governorate of Médenine, located in the southeast of Tunisia (Figure 1). According to the

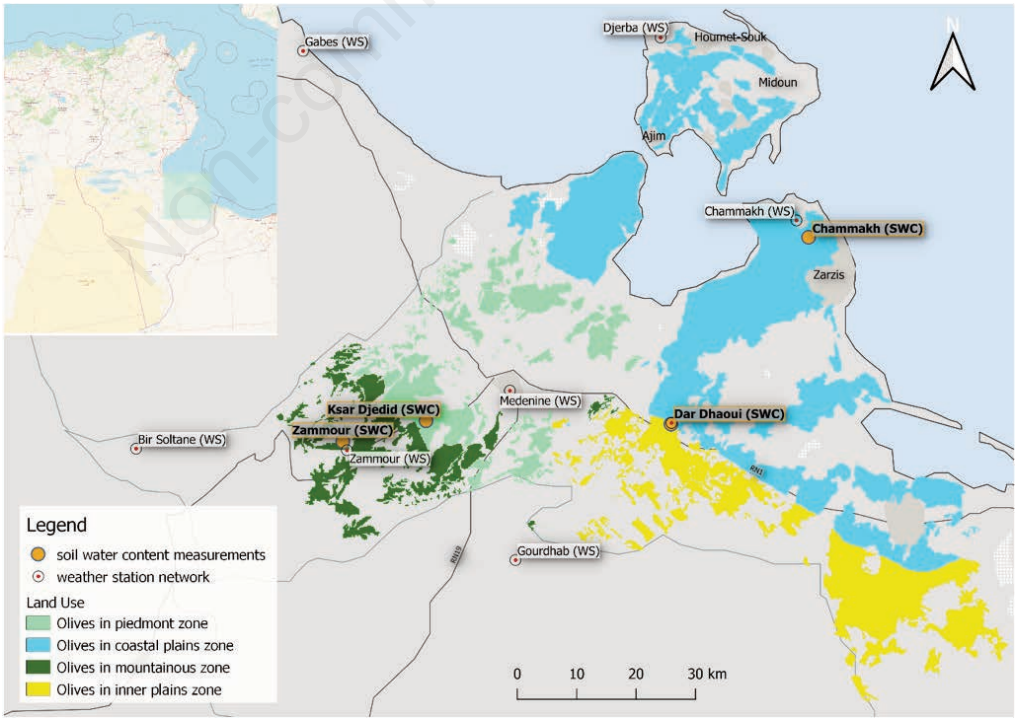

Figure 1. Overview map of the study area, including olive orchards type distribution, weather stations positions, and soil water content measurement locations.

Köppen-Geiger classification system, it is located in low latitude desert climate (BWh - Dry Arid Low Latitudes) (Peel *et al*., 2007). For the most part, the study area has a constant slope toward the Mediterranean Sea, and it covers an area of 8588 km^2. The surface drainage has an intermittent flow regime because of prolonged drought periods. A hot and arid climate characterises the region. The precipitation is irregular, both inter-annual and intra-annually. The average annual rainfall ranges between 240 to less than 150 mm. Due to the rarity of rainfall, the evaporation rate is approximately 1170 mm/year, and it considerably exceeds precipitation for most of the year. In summer, the air circulation is conditioned by the North Atlantic High to the north and the presence of high pressure over the Sahara Desert to the south. In winter, it is governed by the occurrence of North Atlantic highs, Saharan highs, and Mediterranean lows. The mean annual temperature is around 23°C. As for precipitation, the region is characterised by a great fluctuation temperature. During the summer, the maximum temperature can exceed 50°C, and during winter, the minimum temperature can fall below –4°C (Ouessar *et al*., 2006; Latos *et al*., 2018). For the study site, the CRDA-Médenine (2019) estimated that the total available water resources amount to 155.74 million m^3/y, of which 99.08 million m^3/y are actually used for different purposes (mainly (more than 80%) for drinking). Besides, 91% of the land is used in agricultural activities where 28.7% is cultivable, 84% (around 200,000 ha) of which are used to grow olive trees (Sghaier and Ouessar, 2013). As shown in Figure 2, Médenine governorate is characterised by a wide range of soil types. It is mainly covered by isohumic soils (23% of the total area) developed by various climate and vegetation bio-climatic factors (Duchaufour and Duchaufour, 1982). This soil has a relatively high organic matter content with well-developed humus and coarse texture, representing a sandy to sandy-clay texture. It may occasionally have a calcareous crust (Mtimet, 2001). Moreover, we notice the spreading of the poorly evolved alluvial soils. They are rather deep soil with poor organic matter and good drainage, as they have a silty-loam to a sandy texture. The salinity of the soil varies between 0.5 to 3 mS/m according to the specific location, but in general, it appears from bottom to upper layers (Bouaziz and Gloaguen, 2010; Boulbaba *et al*., 2012; Dhaou *et al*., 2014). When the water supply is available, these soils are used for agriculture, more specifically to create an oasis (Mtimet, 2001; Gallali *et al*., 2011). Furthermore, the raw mineral soils types are present predominantly in the Daher plateau and on the slopes of the mountainous chains of Chareb and Matmata. They are hard pebbly plateaus with small traces of organic matter, where most of the sand has been removed by deflation (Latham, 1982). These soils can be either Lithosols or Regosols, depending on the texture. Apart from the scarce desert plants, they are largely deprived of any vegetative cover. They are also used as rangeland (Ayed *et al*., 2018).

Soil water balance modelling

Model description

The HidroMORE model was used to compute the water balance in the olive orchards of the study site. It has been developed to perform a remote sensing-based soil water balance. The model is particularly well adapted to analyse water balance with great spatial variation on large areas. Fundamentally, the calculation of the evapotranspiration in HidroMORE is based on the FAO-56 double-crop coefficient methodology (Allen *et al*., 1998). The calculation treats evaporation (E) and transpiration (T) differently by assigning different coefficients for each component K_e and K_{cb}, respectively, as seen in Equation (1).

$$ET_c = ET_0\,(K_{cb} + K_e) \quad (1)$$

Where ET_0 is the reference evapotranspiration, K_e is the evap-

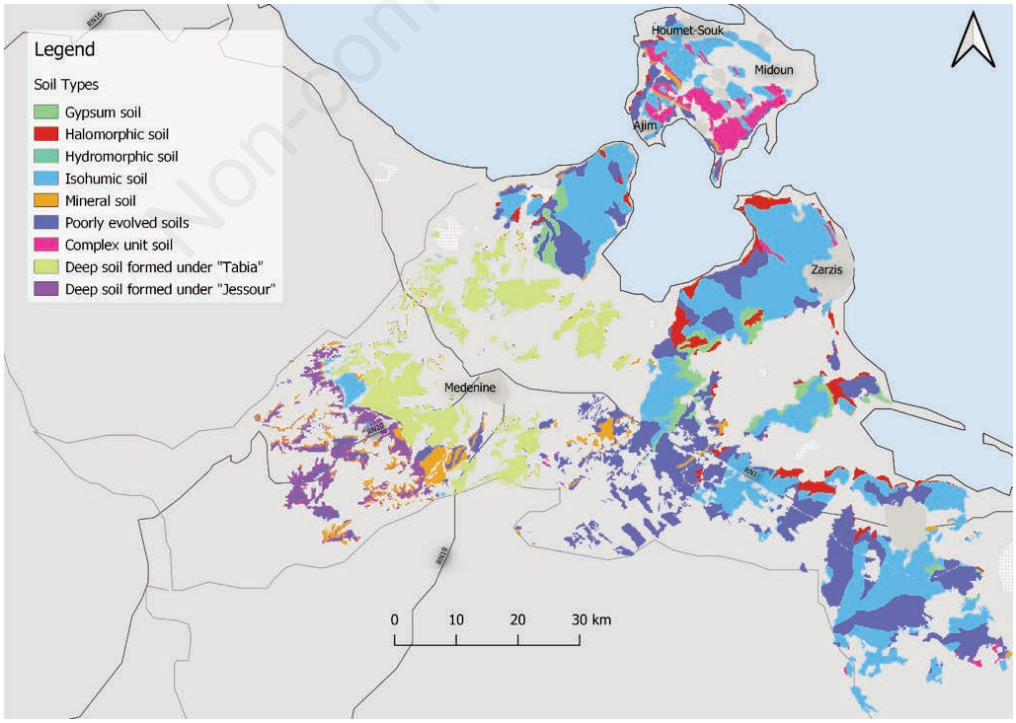

Figure 2. Soil type distribution in the study area.

oration coefficient, and K_{cb} is the basal crop coefficient. K_{cb} is either introduced to the model as daily table input or interpreted from the NDVI map. If interpreted, a linear relation is used to make the estimations, as shown in Equation (2). In this study, we used this equation based on the study of Bausch and Neale (1987) for K_{cb}. Since it used both covered and bare soil to parametrize the equation, it used different plant species and was previously used to estimate K_{cb} for olives in the study area (Hachani *et al*., 2017).

$$K_{cb} = 1.36\,NDVI - 0.03 \quad (2)$$

The model uses both weather station position and daily temperature data from these weather stations to produce an ET_0 map using the inverse of the distance to make spatial interpolations on a daily basis.

The model uses the estimated evapotranspiration to calculate the adjusted evapotranspiration (*Etc*Adj). It is calculated by introducing a coefficient (Ks) to the transpiration component. This coefficient reduces the evapotranspiration proportionally to the water availability (Equation 3).

$$ET_{cAdj} = ET_0\,(K_{cb}K_s + K_e) \quad (3)$$

Ks is equal to 1 if the depletion for the day i-1 is inferior or equal to the readily available water at the soil root depth (RAW) and calculated following the Equation (4) if it is superior to RAW.

$$K_s = \frac{TAW - Dr_{i-1}}{TAW - RAW} \quad (4)$$

Where Dr_{i-1} is the depletion (mm) for the day i-1 (Torres and Enrique, 2010) and TAW is the Total Available Water which is calculated as demonstrated in Equation (5).

$$TAW = 1000 \cdot Zr \cdot (\theta_{FC} - \theta_{WP}) \quad (5)$$

Where Zr is the root depth (m), θ_{FC} is the volumetric water content at Field Capacity (mm), and θ_{WP} is the volumetric water content at Wilting Point (Garrido-Rubio *et al*., 2019).

The model uses the water balance Equation (6). It estimates water balance independently pixel by pixel. It uses NDVI images as input to estimate data related to the plant (such as plant height, K_{cb}, green cover, and root depth). Furthermore, it extrapolates tabular data in dbf file format (precipitation, maximum root depth, irrigation, fraction of vegetative cover, soil characteristics and soil use, and plant height) to produce spatial information in the image format used input layer to the model.

$$Dr_i = Dr_{i-1} - 1 + DP + ETc + RO - P - I \quad (6)$$

Where Dr_i is the depletion (mm) for the day i (Torres and Enrique, 2010), Dr_{i-1} is the depletion (mm) for the day i-1, DP is deep percolation (mm), *Etc* is the evapotranspiration (mm), RO is the runoff (mm), P is the precipitation (mm), and I is the irrigation (mm). This equation is applied for each pixel with a timestep of one day.

Deep percolation was calculated based on the soil data, runoff, and precipitation. The first is given to the model via a map detailing the distribution of soil types across the study area and a table that describes in detail the soil types characteristics. The latter is a map showing the precipitation amount in every pixel. The model produces the map via spatial interpolations using the same method deployed in ET_0. Finally, runoff is calculated using the precipitation map, depletion for the day i-1, and the curve number (CN) map. The latter is produced by a module integrated into the model. Both spatial and characteristics related to soil type and land use are used to calculate the CN map. Specifically, the hydrologic soil group is determined based on field expertise and knowledge according to the guiding principles adopted by the USDA Soil Survey (Neitsch *et al*., 2011). Worth noting that the model estimates the runoff, but it does not take into account any horizontal movement between pixels. Therefore, only direct runoff is considered by the model.

The model calculates the depletion in Equation (6) in the volume defined by the pixel area and root depth. The value is considered homogeneous across both the vertical and horizontal axis.

If a specific pixel result was requested from the model at the start of the simulation, a text file would be generated that provides detailed information about the water budget internal variables at the daily level for the selected pixel. The model provides the volumetric soil water content (SWC) among those variables. It is calculated following the Equation (7).

$$SWC = \frac{(1000\,\theta_{FC}) - Dr_i}{1000} \quad (7)$$

Where θ_{FC} and SWC are in (m^3/m^3), and Dr_i is in (mm).

The model has been applied in various studies. The model was applied to estimate irrigation requirements at the river basin level and large irrigation areas in Spain. The model provides spatial and temporal distribution of the estimations helping with water management and monitoring (Ortega *et al*., 2019; Garrido-Rubio *et al*., 2019, 2020a, 2020b). In particular, the model was applied to a rainfed olive tree in an arid area (Hachani *et al*., 2017).

Model parameterisation

We used the soil map (at 1/200,000 scale) produced by the MAHR (2002). However, in order to account for the additional runoff water collected by the traditional water harvesting techniques resulting in deep soil layers formed behind those structures, we added two specific soil types: Soils behind *Jessour* and Soils behind *Tabias*. For these soil types, the available water capacity, bulk density, and saturated hydraulic conductivity (Table 1) have been parametrised using data from (Ouessar *et al*., 2008, 2009). The readily available water was derived from the water retention curve using data collected by (Taamallah, 2003). Furthermore, the wilting point of these soils has been adjusted from 10 to 6% by volume, considering that in this arid environment, olive trees can extract water from the soil at potentials as low as 7 Mpa (Ennajeh *et al*., 2006). The remaining soil water parameters were estimated using the Saxton soil water characteristic calculator (Saxton and Rawls, 2005). This calculator evaluates soil water characteristics from regression equations developed using readily available variables of soil texture and organic matter from the USDA soil database (Saxton *et al*., 1986; Saxton and Rawls, 2006).

The olive orchards distribution map of the study area is based on the map produced by Sghaier *et al*. (2010). It was further refined and updated by visual interpretation of high-resolution images provided by Google Earth in QGIS. This map classifies four olive orchards types according to the climatic characteristic

and the agronomical practices in the region:

i) *Olives in the coastal plains region:* This area relatively has the most suitable climate for the olive tree, for it has the most precipitation and has a colder temperature in the summer and warmer in the winter due to its proximity to the coast (Dhiab *et al*., 2017). In this region, the tree's canopy is kept moderately sized to enhance olive productivity (Katar *et al*., 2021).

ii) *Olives in the piedmont region:* This region has the typical Mediterranean weather with a rainy season that lasts from September to April. The rainy days are scarce but with high intensity (Ben Fraj *et al*., 2016). That is why we have abundant use of Jessour to help collect the precious rainwater (Castelli *et al*., 2019). Under this system, farmers tend to keep the tree's canopy as large as possible to mitigate evapotranspiration by creating a humid micro-climate under the canopy (Calianno *et al*., 2020).

iii) *Olives in the mountainous region:* This zone has a similar climate to the piedmont region with slight differences. That can be summarized in the higher maximum temperature in the summer, caused by the dry Saharan winds and a higher average annual rainfall because of the higher altitude of the plateau. Most olive plantations are very limited in size and separated due to the rugged topography (Ouessar *et al*., 2009). Almost all of them are under traditional water harvesting techniques called *Tabia*, which has a similar purpose and functionality as the *Jessour*. Hence, similar pruning techniques to those used in the piedmont region are used. However, due to the steeper slopes in this region, more water is collected. So, farmers maximize the tree frame to a greater degree sometimes they fuse several trees into one canopy to reduce evapotranspiration even more (Ouessar *et al*., 2009).

iv) *Olives in the inner plain region*: This zone has a harsher climate due to its position far from the sea and the low elevation. It recorded the highest temperature by a substantial margin during summer and has the lowest average annual rainfall (Mraidi *et al*., 2018). Soil is sandy loamy with high porosity, which limits runoff. Due to the unsuitable and hostile climatic conditions, the tree canopy is reduced to a bare minimum, and the trees are 25-32 m spaced (Magdich *et al*., 2015).

Evaluation of model performance

An evaluation of the model was performed where we ran the model using the 2016 data to initialise the model parameters and estimate the stored water in the soil at the beginning of the following year. Then, to evaluate the results, we compared the model outputs to the measured water content and three consecutive years of campaigns (2017-2019) in the four sites. The targeted results were isolated in time by selecting the correspondent date and location by selecting the appropriate pixel and day. The statistical parameters calculated in order to analyse and compare the results of the soil water content are the minimum (Min), maximum (Max), standard deviation (σ), root mean square error (RMSE), regression coefficient (R^2), and Index of Agreement (IA), which are commonly used in hydrological model evaluations. Each soil moisture measurement was compared to the corresponding pixel in the daily output simulation results. These simulations were taken with a delay of one day to account for any changes occurring on the measurement day.

Model simulation

Water balance simulation using HidroMORE has been performed for the entire olive land-use area of the governorate of Médenine based on the observed inputs for the study period, from January 2016 to December 2019. Data from 2016 were disregarded and considered warming up period for the simulation.

Field collected and satellite data

Soil moisture measurement data

In order to validate and assess the performance of the HidroMORE model, soil moisture data were taken from four rainfed olive orchards within Médenine governorate: Zarzis, Dar Dhaoui, Ksar Jedid, and Zammour (Figure 1), representing respectively the main agro-ecological zones of the study site: coast, inner plains, piedmont, and mountains. The soil moisture measurements were performed over four years with no data for 2018 (2016, 2017, and 2019) at a monthly frequency and after each rainfall event. Sometimes, the measurements became less frequent due to field limitations that did not allow more frequent readings. For each reference site, 60 soil samples were taken every 20 cm over a depth of 1 m using the gravimetric method (Myhre and Shih, 1990). Then, these collected samples were weighed and placed in the hot-air oven and dried at 105°C temperature for 24 hours (Aniley *et al*., 2018). Finally, the change in soil weight before and after drying was used to calculate the water content of the soil volume. The value for each reference site was the average of the 12 measurement points within 6 m radius around 3 selected olive trees (Figure 3).

Table 1. Description of the soil inputs parameters used by the model.

Parameter	Description	Estimation method description	Reference
REW	Readily available water in soil	Derived from the water retention curve	Taamallah, 2003
Ze	Depth of the evaporation active layer soil	Data were extracted from the soil map	MAHR (2002)
Pr_limitan	Limiting depth for roots	Data were extracted from the soil map and adjusted to more depth in the Tabia and Jessour soil type	MAHR (2002)
WP	Wilting point in volumetric humidity	Derived from the water retention curve and adjusted to consider the capability of olive trees of extracting water from lower soil at potentials	Ennajeh *et al*., 2006 and Taamallah, 2003
Fc	Field capacity	Estimated using the Saxton soil water characteristic calculator*	Saxton and Rawls, 2005 and Ouessar *et al*., 2008, 2009
Sat	Saturation point	Estimated using the Saxton soil water characteristic calculator*	Saxton and Rawls, 2005 and Ouessar *et al*., 2008, 2009
K	Saturated hydraulic conductivity	Estimated using the Saxton soil water characteristic calculator*	Saxton and Rawls, 2005 and Ouessar *et al*., 2008, 2009

*Parametrised using data from Ouessar et al. (2008, 2009) for soils behind Jessour and Soils behind Tabias.

Climatic data

Except for the Médenine weather station owned by the National Institute of Meteorology (INM), daily climatic data (namely precipitation and temperature) were collected from the IRA's climatic network. The network has a grid of weather stations in and around the study area. This study used data from eight weather stations located in and around the study zone (Figure 1).

Satellite data

18 cloud-free Sentinel-2 images, acquired between June 2016 and December 2019 over Médenine governorate, were used (one image for each season). Both level-1C and Level-2A images were downloaded from the Copernicus Open Access Hub (https://scihub.copernicus.eu/dhus/#/home) and the USGS Earth Explorer platform (https://earthexplorer.usgs.gov).

The L1C products were atmospherically corrected based on the Sen2Cor plugin of the SNAP Software to obtain the surface reflectance L2A product (Louis *et al*., 2016). According to the requirement of this research, the normalized difference vegetation index (NDVI) was computed, with band 4(RED) and band 8 (NIR) of Sentinel 2 data, using the Equation (8).

$$NDVI = \frac{(NIR-RED)}{(NIR+RED)} \quad (8)$$

Results

Meteorological context and significant rainfall events

The hottest day of the year occurs in June and July for all weather stations. The highest maximum temperature recorded was 49°C in Bir Soltan, Chammakh, and Dar Dhaoui. However, the highest mean annual maximum temperature (26°C) was recorded in 2017 at Gordhab station.

During the experiment, only two rain events that exceeded 100 mm were recorded both in 2017, the first (145 mm) happened in April, and it affected only the region of Zammour, the second (116 mm) happened in November, and it was less localised as it affected the regions of Médenine, Djerba, and Chammakh. On average, Chammakh, Zammour, Médenine, and Djerba received more rain annually. In contrast, Dar Dhaoui station received the least annual rainfall of all the stations.

Figure 4 shows the maximum and minimum average monthly temperature and the cumulative monthly precipitation of all the regions. As we can see in Figure 4, the 2017-2018 campaign was the rainiest year, but as stated earlier, this higher number can be attributed to two heavy rain events that might trigger an intense runoff. The temperature was typical of the region, with no noteworthy annual differences.

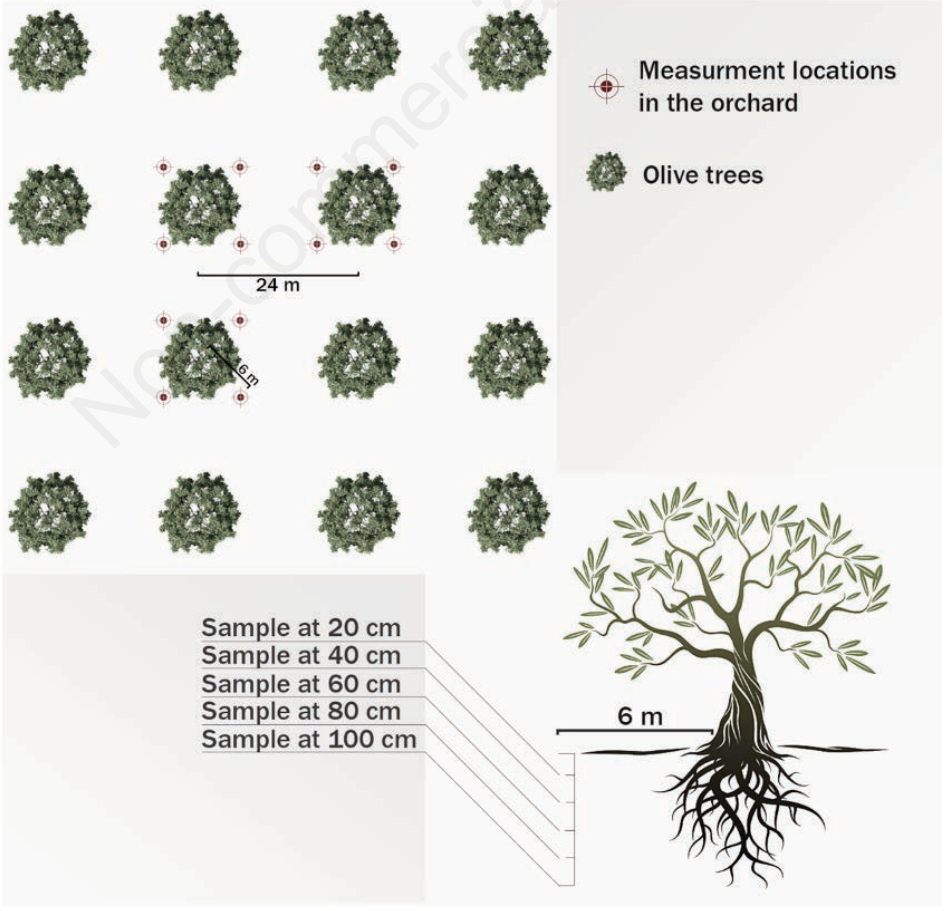

Figure 3. Soil measurements position in the orchards.

Validation results

Table 2 shows the comparison between the measured soil water content and the simulation results. During the three years of the experiment, the P-values for all the linear regressions are smaller than 0.05 therefore all linear regressions are statistically significant. The estimated soil water content showed a strong regression coefficient r^2 for both zones of Zammour and Ksar Djedid (0.92 and 0.77, respectively) and a strong index of agreement (0.91 and 0.72, respectively). However, the soil moisture of the zones of Zarzis and Dar Dhaoui has a smaller correlation (with R^2 equal to 0.59 and 0.52 for Zarzis and Dar Dhaoui, respectively).

In general, the model overestimates the soil water content. This is evident when the data from all regions are combined and in the individual regions. When analysed region by region, we can see that the model slightly overestimates the soil water content in the mountainous and piedmont regions, *i.e.*, when there is a strong correlation. However, this was not the case for Zarzis and Dar Dhaoui, where the model showed a more significant overestimation. For the most part, the index of agreement was in concordance with the regression coefficient. At its highest (0.91 in Zammour), the model strongly agrees with the measurements. At its lowest (0.67 in Dar Dhaoui), the model still produces a reasonable prediction.

In addition, despite the substantial variability between the zones, shown in the maximum and minimum values for each region, the model estimates the water soil content relatively with satisfactory accuracy for each zone. These results emphasize the flexibility of the model across the different regions. For example, the mountainous region recorded almost double the maximum soil water content of the inner plain region. When it comes to the minimum soil water content, the difference was more staggering, where the Zammour region recorded nearly the triple soil moisture recorded in Dar Dhaoui. Overall, when all regions were combined, the model showed good regression and agreement values (0.72 and 0.76, respectively).

Simulation results

In order to illustrate the result of the simulation in the case of land surfaces covered with olive-tree, Figure 5 shows the evolution of the olive-covered area by the simulated depletion classes in the monthly time step. The precipitation input data are shown at the bottom row, which shows the inner-annual (seasonal) ups and downs typical for the region. Water depletion follows this cycling closely throughout the years, which is shown by the expansion of the area with low depletion in rainy seasons and vice versa. The only notable exception of this was in the early summer of 2019, when precipitation had almost no effect on the area distribution. This strong correlation between water depletion and rainfall can also be seen on a yearly basis. As the annual precipitation decreased from 2017 to 2019, we can notice the expansion of the areas with heavy water depletion. As the drought became more severe, the autumnal rains could not replenish the water reserve in

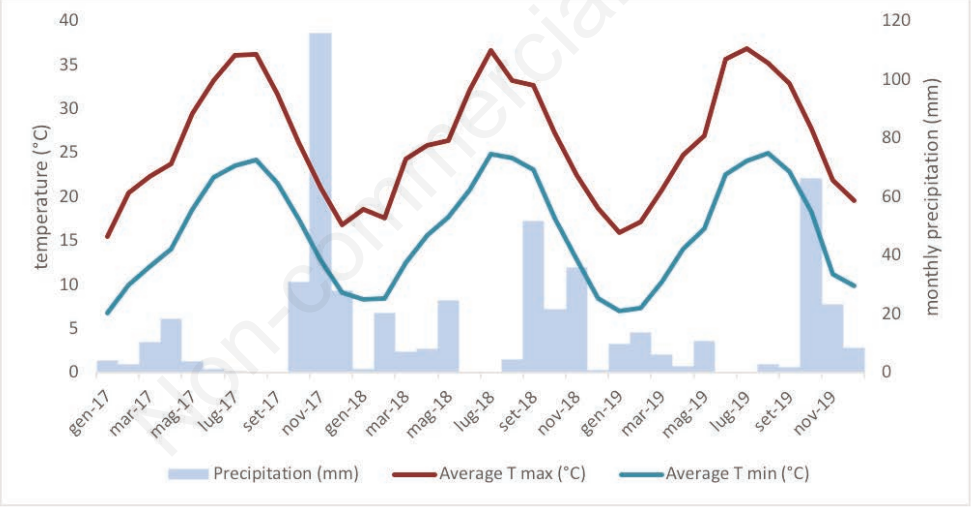

Figure 4. Interstation average monthly precipitation, maximum and minimum temperatures (T max and T min) during the observation period in the study site.

Table 2. Comparison between estimated and measured soil water content in the four agro-ecological zones of the study site during the observation period.

	R^2	P-value	IA	RMSE (mm)	Min (mm)	Max (mm)	St. dev. (σ)
Zammour	0.922	0.0002	0.914	34.9	125	236	15.3
Zarzis (Chammakh)	0.596	0.008	0.718	45.1	25	132	10.2
Ksar Djedid	0.7747	0.0007	0.7299	42.7	44	153	16.5
Dar Dhaoui	0.5212	0.0001	0.6701	44.3	42	128	7.36
All	0.7295	5.2E-15	0.7697	40.3	25	236	25.7

IA, index of agreement; St. Dev., standard deviation.

the soil profile. Figure 6 shows the evolution of the olive areas affected by severe drought (depletion higher than 150 mm) compared to the average depletion of the olive area in the region at a monthly time step. As can be seen in Figure 6, while the effect of seasonal variation can be noticeable in both parameters, the annual variation has affected them differently. Hence, drought expanded the vulnerable area dramatically but did not have a strong significance on the average depletion.

In rainfed orchards, soil water balance depends on rainfall as the main source of water supply and on evapotranspiration as the most important component in terms of extracting water from the topsoil layer. The water stress coefficient (K_s) offers an insight into the effect on the tree independently from the evaporation component (Kokkotos *et al*., 2020). For an overview of the general spatial distribution of these simulated parameters, corresponding simulation results in yearly pace have been summarised in Figure 7.

Soil water depletion is the product of all the factors combined. However, we can see that precipitation has the most significant share of influence. This can be seen as even regional rainfalls can reverse the general trend; for instance, a localised rainfall of 70 mm in 2018 in the region of Médenine restored the water reserve and thus reduced the water depletion in that area, when all other regions appear to be affected by the general drought in 2018.

As shown in Figure 7A, the precipitation amount has the biggest share of influence over the soil water depletion, as we can see that areas with high depletion levels expanded in the years with low total precipitation. Furthermore, when we compare the precipitation map and depletion level, we can see a clear overlap of these

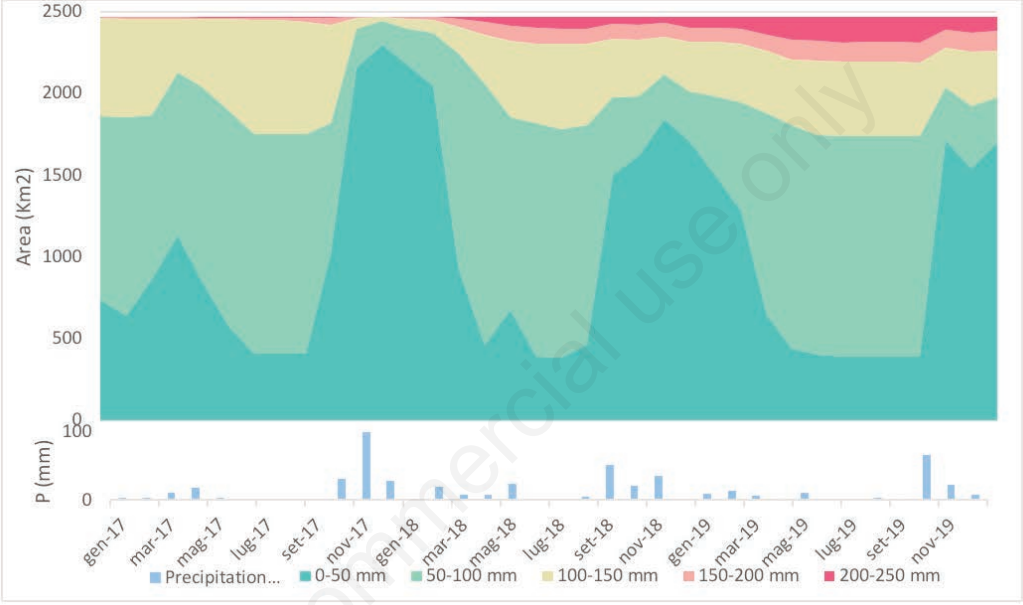

Figure 5. Evolution of the olive planted area (km²) in the study site by depletion classes - during the observation period.

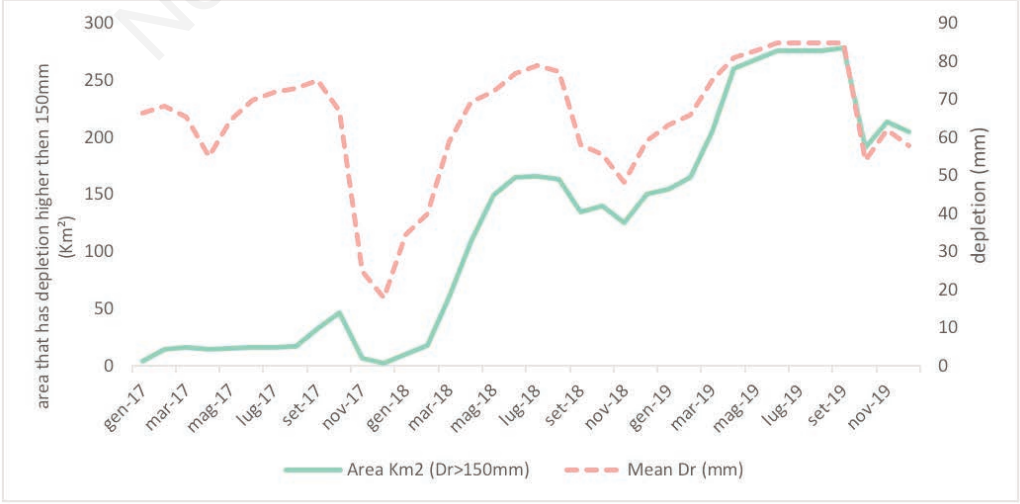

Figure 6. Evolution of the olive planted area (km²) with depletion higher than 150 mm in the study site and the mean monthly depletion (mm) during the observation period.

two maps. Similarly, a comparison between soil map and depletion shows that poorly evolved soils with low water retention capability increased the water depletion. Figure 7 shows that olive growing zones were dynamic over the simulation period. As such, in the mountainous and the piedmont regions, the model generated low water depletion even in 2018 and 2019. In inner plain and coastal regions, the model produced a mosaic pattern of water depletion levels during drought.

Figure 7B shows an increase in stress coefficient as we move away from the coast. Additionally, we can note significant variability in stress levels in the mountainous zone. On the contrary, the stress level in the coastal zone was more or less homogenous spatially. Figure 7C shows the annual spatial distribution of the adjusted evapotranspiration. It shows that overall adjusted evapotranspiration was high in the mountainous zone. Conversely, it was relatively low for the inner plain zone; these low values ranged between 163 and 337 in 2017 and 219 and 419 in 2018.

Figure 8 illustrates the percentage of the olive growing area where the stress coefficient is below 0.25 by olive growing region at a monthly time step. It shows a high seasonal variability across all the regions. Excluding June and July of 2019, Figure 8 shows a substantial variability between olive growing zones. For example,

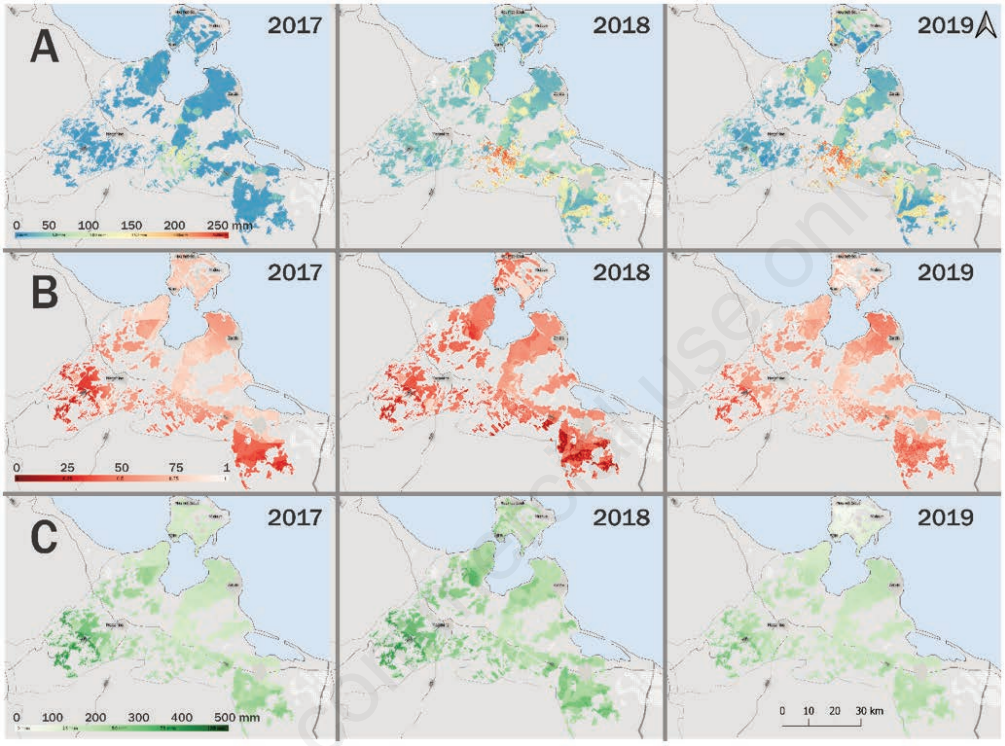

Figure 7. Average simulated annual: soil water depletion (mm) (A), stress coefficient (dimensionless) (B), and adjusted evapotranspiration (mm) (C) during the observation period in the study site.

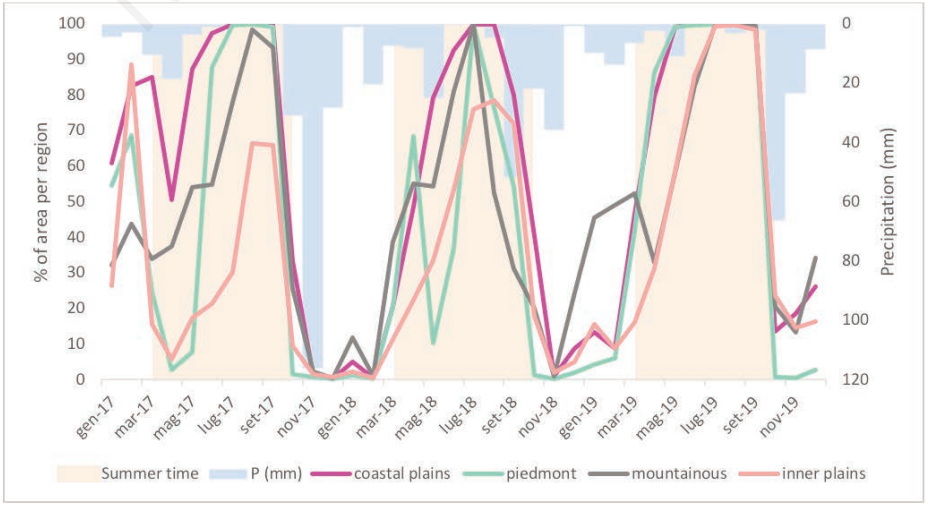

Figure 8. Percentage of the area where the stress coefficient is extreme (0->0.25) by olive growing region.

the mountain zone has a shortened and delayed phase of stress during the summer. On the other hand, data show that the olive area was not totally under severe stress in inner plain olive orchards until later in 2019.

Figure 8 shows that during the relatively short period of drought (2 years), almost all olive plantations, regardless of the zone, fall entirely under severe stress. While this condition is reverted as soon as the summer season ends, we can notice a varying degree of response depending on the zone and the year.

Discussion

Model evaluation

Since modelling plant-soil water balance is complicated, it is common for soil water models such as SPARSE, SAMIR, METRIC, and MINARET to have a small margin of inaccuracy when estimating soil moister (Santos *et al*., 2012; González-Dugo *et al*., 2013; Saadi *et al*., 2015, 2018). Depending on the methodology utilised in each study, this inaccuracy can often be attributed to poor configuration of soil layers, incorrectly calibrated inputs, and inadequate temporal or spatial nature of the input data. Our study noticed a persistent overestimation of the soil water balance across the regions. In previous studies that used HidroMORE as a modelling platform, this overestimation of soil water content was attributed to two factors (Sánchez *et al*., 2010):

i) The presence of sandy soils (and soils with high infiltration coefficient in general) can increase the rate of deep percolation, and if not accounted for, this can off-balance the model calculation in favour of more water retention thus an overestimation of the simulated soil water content. In the study zone, these types of soils are abundant and cover extensive areas (Mtimet, 2001). However, in many cases, these soils are completely misidentified or not described correctly. This could be seen when actual soil analysis was taken. Frequently, analysis results disagree with the described soil type in the map (Schiettecatte *et al*., 2005; Dhief *et al*., 2011; Nagaz *et al*., 2012).

ii) The root depth of the crop can have a great impact on the soil water content estimation. It defines the soil volume in which the plant can extract the water via transpiration. If the actual root depth is greater than the model input, the real tree has more water available to extract from the additional volume. Thus, the real plant-soil system will lose more water to the environment through transpiration, and we will overestimate the soil moisture in part of the model. In the case of the olive tree under rainfed conditions, this parameter can be particularly hard to define (Connor, 2005). It varies from less than a metre in shallow soil with near-the-surface soil crust to more than 3 m, depending on the soil characteristic, water availability pattern, and cultivar (Nguyen and Bich, 2019). The distribution of the root system of the olive tree is adaptive on both the vertical and lateral axis (Tognetti *et al*., 2005; Zeleke, 2014). Particularly, root development is very responsive to water supply in rainfed systems and can exceed the normal root development by a substantial margin (Connor, 2005). In this study, the diversity of soil types, water harvesting techniques, and the occasional supplementary irrigation favour a diverse root system. In addition, olive trees are grown from both seedlings and cuttings, which further deepen the root diversity (Connor, 2005). Despite our effort to classify olive orchards in four different zones, the variability within the zones and the extent of the olive root system were underestimated in this study (Rouina *et al*., 2007).

Furthermore, HidroMORE tends to underestimate the irrigation requirement during the summer (which is inversely proportional to the soil water content) for different crops (Garrido-Rubio *et al*., 2020a). This was due to the underestimation of evapotranspiration. The underestimation is intrinsic to the method used by HidroMORE to calculate evapotranspiration, which is the FAO56 dual crop coefficient (Moreno *et al*., 2017; Garrido-Rubio *et al*., 2020a). This method appears to systematically underestimate reference evapotranspiration in semi-arid and windy areas with high atmospheric evaporative demand (Fernández *et al*., 2010).

The overall relatively low correlation observed between the model output and measured data is due to the methodology of this study that uses soil moisture as the parameter to validate the result. Soil moisture is sensitive to a wide range of environmental factors. Thus, accurately estimating it with a narrow margin of error is still a major challenge (Karandish and Šimůnek, 2016; Hati *et al*., 2020). Furthermore, when compared to measured soil water content, reported a correlation of this parameter in similar studies is often low, and the correlation coefficient (r^2) ranges between 0.17 and 0.84 (Wagner *et al*., 2007; Elshorbagy and Parasuraman, 2008; Yinglan *et al*., 2019). However, this parameter offers insight into the real performance of the model since it evaluates the most difficult parameter to estimate in the water balance equation that can be measured relatively easily on the field (Sheets and Hendrickx, 1995).

We can notice that the correlation coefficient (R^2) is in concordance with the index of agreement; this is to be expected as the latter is a natural extension to the former. However, the index of agreement highlights the bias encountered in the data and eliminates the effect of group size (Cohen *et al*., 2001; Duveiller *et al*., 2016). Thus, the slightly better index of the agreement shows that even when the correlation is weak, the datum is symmetrical and interchangeable. Therefore, the model prediction shows minimum bias between low soil water content data and high ones. Regardless of the statistical metrics, the model better predicts soil water content for Zammour and Ksar Djedid. This can be attributed to the specific soil types occupied by olive orchards in these zones. As discussed previously, soil type is a major factor in the erroneous result for HidroMORE, and when this issue is addressed, we minimise error factors. In these zones, soil characteristics were obtained from the previous field and/or laboratory measurements. This adjustment gave the model better inputs to simulate the soil water retention. In addition, the deep soil layer allowed a deeper root zone by eliminating the inherited limit of soil depth. Hence, the model simulated more water loss via evapotranspiration in the absence of rain. On the other hand, the low correlation in the coastal and inner plains shows that a finer soil map with better soil characteristics is crucial to improve simulation results.

The model showed satisfactory results across all zones, highlighting the model's robustness despite the high spatial variability.

Model simulation

In the early summer of 2019, recorded precipitation appears to have no visible effect on the modelled depletion. This abnormality can be explained by misrepresenting the real amount of rain in that period. A very spatially limited rain event that falls on one of the weather stations can overestimate the precipitation input when the model extrapolates the punctual weather station data to the nearby area (Moreno *et al*., 2017). This limitation can be solved by increasing the density of weather stations.

The depletion level follows the annual drought patterns. Hence, the depletion was not so severe in the first two years, but it became more extreme by mid-2019. The water reserve was quickly

restored as soon as the autumn entered; thus no permanent damage was inflicted on the trees. However, the implication of the extreme depletion of the water reserve on the yield will manifest in the following harvest by prolonging the period of no production. While it is normal for orchards to be harvested once in three or four years, with the increased economic pressure, farmers may abandon these traditional orchards due to low productivity (Khabou *et al*., 2009). This can have profound consequences on the already fragile social integrity of the region. Moreover, this spike in depletion can be an early warning to prepare for supplementary irrigation in the next year to avoid permanent damage to the trees.

The spatial distribution of water depletion reveals the effect of soil type, and this can be clearly seen in the region near Dar Dhaoui, where the presence of the poorly evolved soil type with low water retention capacity increased the water depletion in all the simulation period (Mtimet, 2001; Taamallah, 2003). However, the mountain and the piedmont zones maintained low water depletion even in 2018 and 2019. In there, the added water by the traditional water harvesting systems contributed to combatting the low precipitation. This shows the importance of these structures, which are highlighted in several studies (Ouessar *et al*., 2006, 2008, 2009; Ben Fraj *et al*., 2016; Castelli *et al*., 2019; Calianno *et al*., 2020). These results emphasize once again the effectiveness of these traditional techniques and the importance of incentivising farmers to install them (Adham *et al*., 2019).

In lowland regions, we can see a mosaic of water depletion levels during the drought; this variability follows the soil type map. This stresses the importance of using high resolution and accurate maps in simulations to guide the decision-making processes regarding the region. The generated variability from soil heterogeneity is observed in other HidroMORE applications (Ortega *et al*., 2019), which weigh the model's suitability in such a complex environment. In the study area, we had limited options when choosing the soil map for the simulation. Hence, a more detailed and updated map is needed for better results in the Médenine governorate. At the monthly time step (data not presented), we can see that throughout the years, the mountain and the piedmont zones were the most affected during the summer. This can be seen in water depletion levels in these regions. This is due to the relatively higher evapotranspiration generated in those regions (Calianno *et al*., 2020). However, with the rainy season onset (autumn), trees could recover, as shown by the reduced water depletion. In the inner plain region, despite the hot and arid climate, seasonal change was less detrimental than the yearly change; this is most likely due to the measures taken by farmers to adapt trees to the stressful conditions. Thus, the horticultural practices lessened the effect of harsh climate (Karray and Abichou, 2007). In coastal olives, the proximity to the sea reduces the severity of the climate. Thus, while the depletion rate increased during the summer, the increase was moderate. Worth noting that the coastal area has the lion's share in olive production in the region (ODS, 2019). Thus, any measure taken to improve olive productivity will have the most significant impact on the gross olive production. In both these regions, precipitation has a more immediate effect on depletion (Dhaou *et al*., 2009).

The spatial distribution of the adjusted evapotranspiration and the stress coefficient is mainly influenced by the climate, soil, and olive orchards type. In the latter case, this can be seen by the increase of stress level as we move away from the coast, where the climate can be harsher. The mountainous zone stood out with significant variability in the simulated stress level regardless of the year; this can be attributed to the heterogeneous terrain characterized by the presence of steep slopes and variation in altitudes (Ouessar, 2017). However, the coastal olive region seems to be the most sensitive to weather conditions as stress levels appear more or less homogenous across the region but differ remarkably from year to year. On the other hand, the effect of olive orchards type on evapotranspiration can be seen in mountainous and piedmont regions where the combination of large size of the tree canopy produces higher rates of transpiration and the higher evaporative demand create greater evapotranspiration rates. In the inner plain olive orchards, we can see that despite the zone's high evaporative demand, the adjusted evapotranspiration remained relatively. In this region, the horticultural practices well adapted to extremely stressful conditions can explain these low values (Karray and Abichou, 2007).

As shown previously, all regions showed clear seasonal variability, with a strong influence on the amount of precipitation. Except for the summer of 2019, we can see substantial variability between olive growing zones. This inconsistency can be attributed in part to localized regional rainfall. However, throughout the experiment and regardless of local rainfall, the mountainous regions have a shortened and delayed phase of stress during the summer, where the majority of olive allocated land is under severe stress. Another remarkable trend appears with inner plain olive orchards, where the olive area is not totally under severe stress until later in 2019. The coastal olives were the most affected by stress. This can be seen in the extended period of time when the olive area is in totality under severe stress.

Conclusions

This study aimed to map the spatial distribution of drought stress in the olive groves in the governorate of Médenine through the computation of the water balance in the olive orchards of the study site using the HidroMORE model. The study's results confirm the reliability of the remote sensing-based soil water balance estimation as a tool for monitoring olive trees over a large and diverse area in arid and semi-arid conditions. It was capable of detecting variation at the orchard level. Besides, it has a reasonable accuracy across all the regions, despite the vast difference in climate, topography, agricultural practices, and cultivars. Moreover, the input required for the methodology used in this study was minimal and readily available. This approach can be used over a larger area and can be used on a national or regional level (MENA or North Africa) to create a unified system of evaluation. This can help organize actions and government intervention in order to increase sustainability.

This study corroborated many studies' findings that the traditional water harvesting system is an effective tool in reducing the effect of aridity on the olive trees. Furthermore, it indicated that selecting the appropriate soil type is crucial in lessening the impact of water shortage during drought. As such, performing soil analysis is highly l to assess productivity and evaluate the likelihood of tree survival. This is particularly important in the coastal region where tree productivity is high, and the weather is more favourable for olive production. In the inner plain olive zone and despite the extreme harsh weather, olive trees were horticulturally conducted to reduce the effect of stress. While the productivity is marginal, the social importance of these plantations justifies the effort to save them in a period of prolonged drought.

Moreover, all olive plantations, regardless of the zone, fall entirely under severe stress by the end of 2019. This shows that during an extended period of drought, intervention is required to

save the trees. Hence, prioritising areas of intervention is mandatory. In that sense, our study offers an objective tool to prioritise orchards in an eventual intervention. Furthermore, the work presented in this study can be extended via linking the water balance model with climate models for future forecasts and seeking more opportunities in CC's framework.

References

Abazi U., Lorite I.J., Cárceles B., Raya A.M., Durán V.H., Francia J.R., Gómez J.A. 2013. WABOL: A conceptual water balance model for analyzing rainfall water use in olive orchards under different soil and cover crop management strategies. Comput. Electron. Agric. 91:35-48.

Adham A., Wesseling J.G., Abed R., Riksen M., Ouessar M., Ritsema C.J. 2019. Assessing the impact of climate change on rainwater harvesting in the Oum Zessar watershed in Southeastern Tunisia. Agric. Water Manag. 221:131-40.

Allen R.G., Pereira L.S., Raes D., Smith M. 1998. Crop evapotranspiration-Guidelines for computing crop water requirements-FAO Irrigation and drainage paper 56. FAO, Rome 300:D05109.

Aniley A.A., Naveen Kumar S.K., Akshaya Kumar A. 2018. Review article soil moisture sensors in agriculture and the possible application of nanomaterials in soil moisture sensors. Int. J. Adv. Eng. Res. Technol. 6:134-42.

Ayed B., Jmal I., Sahal S., Bouri S. 2018. The seawater intrusion assessment in coastal aquifers using GALDIT method and groundwater quality index: the Djeffara of Medenine coastal aquifer (Southeastern Tunisia). Arab. J. Geosci. 11:1-19.

Bausch W.C., Neale C.M.U. 1987. Crop coefficients derived from reflected canopy radiation: a concept. Trans. ASAE 30:703-9.

Besnard G., Bervillé A. 2000. Multiple origins for Mediterranean olive (Olea europaea L. ssp. europaea) based upon mitochondrial DNA polymorphisms. Comptes Rendus l'Académie des Sci. III-Sciences la Vie 323:173-81.

Bouaziz S., and Gloaguen R. 2010. Surface features analysis in salt-affected area using hyperspectral data: a case study in the zone of Chott, Tunisia. Available from: https://www.researchgate.net/publication/297738490

Boulbaba A., Marzouk L., ben Rabah R., Najet S. 2012. Variations of natural soil salinity in an arid environment using underground watertable effects on salinization of soils in irrigated perimeters in South Tunisia. Int. J. Geosci. 3:1040-7.

Calianno M., Fallot J.-M., Fraj T. Ben, Ouezdou H. Ben, Reynard E., Milano M., Abbassi M., Messedi A.G., Adatte T. 2020. Benefits of water-harvesting systems (Jessour) on soil water retention in Southeast Tunisia. Water 12:295-310.

Cammalleri C., Agnese C., Ciraolo G., Minacapilli M., Provenzano G., Rallo G. 2010. Actual evapotranspiration assessment by means of a coupled energy/hydrologic balance model: Validation over an olive grove by means of scintillometry and measurements of soil water contents. J. Hydrol. 392:70-82.

Castelli G., Oliveira L.A.A., Abdelli F., Dhaou H., Bresci E., Ouessar M. 2019. Effect of traditional check dams (jessour) on soil and olive trees water status in Tunisia. Sci. Total Environ. 690:226-36.

Cohen A., Doveh E., Eick U. 2001. Statistical properties of the rWG (J) index of agreement. Psychol. Methods 6:297-313.

Connor D.J. 2005. Adaptation of olive (Olea europaea L.) to water-limited environments. Aust. J. Agric. Res. 56:1181-9.

Dhaou H., Bouzaida D., Taâmallah H., Ouessar M. 2014. Apport des données Landsat Thematic Mapper pour la cartographie des sols dans la région de Menzel Habib. In: Dhaou H., Ouerchefani D., Taamallah H., Donald G., and Ouessar M. 2009. Drought impact on the olive-trees in the Tunisian Jeffara. J. Arid L. Stud. 19:331-4.

Dhiab A.B., Mimoun M.B., Oteros J., Garcia-Mozo H., Domínguez-Vilches E., Galán C., Abichou M., Msallem M. 2017. Modeling olive-crop forecasting in Tunisia. Theor. Appl. Climatol. 128:541-9.

Dhief A., Abdellaoui R., Tarhouni M., Belgacem A.O., Smiti S.A., Neffati M. 2011. Root and aboveground growth of rhizotron-grown seedlings of three Tunisian desert Calligonum species under water deficit. Can. J. Soil Sci. 91:15-27.

Duchaufour P., Duchaufour P. 1982. Soils with matured humus: isohumic soils and vertisols. pp. 236-269 in Pedology. Springer, Netherlands. Available from: https://link.springer.com/chapter/10.1007/978-94-011-6003-2_9 Accessed: August 21, 2020.

Duveiller G., Fasbender D., Meroni M. 2016. Revisiting the concept of a symmetric index of agreement for continuous datasets. Sci. Rep. 6:1-14.

Elshorbagy A., Parasuraman K. 2008. On the relevance of using artificial neural networks for estimating soil moisture content. J. Hydrol. 362:1-18.

Ennajeh M., Vadel A.M., Khemira H., Ben Mimoun M., Hellali R. 2006. Defense mechanisms against water deficit in two olive (Olea europaea L.) cultivars 'Meski'and 'Chemlali.' J. Hortic. Sci. Biotechnol. 81:99-104.

Estrada F., Botzen W.J.W., Calderon-Bustamante O. 2020. The Assessment of Impacts and Risks of Climate Change on Agriculture (AIRCCA) model: a tool for the rapid global risk assessment for crop yields at a spatially explicit scale. Spat. Econ. Anal. 15:262-79.

Fernández-Escobar R., De la Rosa R., Leon L., Gomez J.A., Testi L., Orgaz F., Gil-Ribes J.A., Quesada-Moraga E., Trapero A., Masallem M. 2013. Evolution and sustainability of the olive production systems. Options Mediterr. 106:11-42.

Fernández-Uclés D., Elfkih S., Mozas-Moral A., Bernal-Jurado E., Medina-Viruel M.J., Abdallah S.B. 2020. Economic efficiency in the tunisian olive oil sector. Agriculture 10:391-411.

Fernández M.D., Bonachela S., Orgaz F., Thompson R., López J.C., Granados M.R., Gallardo M., Fereres E. 2010. Measurement and estimation of plastic greenhouse reference evapotranspiration in a Mediterranean climate. Irrig. Sci. 28:497-509.

Ferreira M.I. 2017. Stress coefficients for soil water balance combined with water stress indicators for irrigation scheduling of woody crops. Horticulturae 3:0-38.

Fraga H., Moriondo M., Leolini L., Santos J. A. 2021. Mediterranean olive orchards under climate change: a review of future impacts and adaptation strategies. Agronomy 11:0-56s.

Ben Fraj T., Abderrhahmen A., Ben Ouezdou H., Reynard E., Milano M., Calianno M., Fallot J.-M. 2016. Les Jessour dans le Sud-est tunisien: Un système hydro-agricole ancestral dans un milieu aride. pp. 193-198 in Climat et pollution de l'air. Actes du XXIXe colloque de l'Association Internationale de Climatologie, 6-9 juillet 2016, Besançon, France.

Gallali T., Brahim N., Bouajila A., Bernoux M. 2011. Spatial distribution of soil organic carbon stock in Tunisia. JOURNAL? VOLUME?:283-9.

Garrido-Rubio J., Calera A., Arellano I., Belmonte M., Fraile L., Ortega T., Bravo R., and González-Piqueras J. 2020a. Evaluation of remote sensing-based irrigation water accounting at river basin district management scale. Remote Sens. 12:3187-215.

Garrido-Rubio J., González-Piqueras J., Campos I., Osann A., González-Gómez L., Calera A. 2020b. Remote sensing–based soil water balance for irrigation water accounting at plot and water user association management scale. Agric. Water Manag. 238:106-18.

Garrido-Rubio J., Sanz D., González-Piqueras J., Calera A. 2019. Application of a remote sensing-based soil water balance for the accounting of groundwater abstractions in large irrigation areas. Irrig. Sci. 37:709-24.

Gómez J.A., Rodríguez□Carretero M.T., Lorite I.J., Fereres E. 2014. Modeling to evaluate and manage climate change effects on water use in Mediterranean olive orchards with respect to cover crops and tillage management. Pract. Appl. Agric. Syst. Model. Optim. Use Ltd. Water 5:237-65.

González-Dugo M.P., Escuin S., Cano F., Cifuentes V., Padilla F.L.M., Tirado J.L., Oyonarte N., Fernández P., Mateos L. 2013. Monitoring evapotranspiration of irrigated crops using crop coefficients derived from time series of satellite images. II. Application on basin scale. Agric. Water Manag. 125:92-104.

Hachani A., Ouessar M., Zerrim A. 2017. A study of water stress on olive growing under the effect of climate change in South East of Tunisia. pp. 1-16 in Water and land security in drylands. Springer, The Netherlands.

Hajji S., Karoui S., Nasri G., Allouche N., Bouri S. 2021. EFA-CFA integrated approach for groundwater resources sustainability in agricultural areas under data scarcity challenge: case study of the Souassi aquifer, Central-eastern Tunisia. Environ. Dev. Sustain. 23:12024-43.

Hati J.P., Goswami S., Samanta S., Pramanick N., Majumdar S.D., Chaube N.R., Misra A., Hazra S. 2020. Estimation of vegetation stress in the mangrove forest using AVIRIS-NG airborne hyperspectral data. Model. Earth Syst. Environ. 7:1-13.

Huang D., Wang J., Khayatnezhad M. 2021. Estimation of actual evapotranspiration using soil moisture balance and remote sensing. Iran. J. Sci. Technol. Trans. Civ. Eng.:1-8.

Karandish F., Šimůnek J. 2016. A comparison of numerical and machine-learning modeling of soil water content with limited input data. J. Hydrol. 543:892-909.

Karray B., Abichou M. 2007. Fonctionnement, performances et devenir des exploitations oléicoles privées à Médenine (Tunisie). Rev Trop. 25:26-30.

Katar A., Aichi H., Essifi B.(Eds). 2021. Monitoring of land use-land cover changes and assessment of soil degradation using landsat TM and OLI data in Zarzis Arid Region. Environ. Remote Sens. GIS Tunis. Springer International Publishing, Chapter 11, pp. 213-31.

Khabou W., Amar F. Ben, Rekik H., Beghir M., Touir A. 2009. Performance evaluation in olive trees irrigated by treated wastewater. Desalination 246:329-36.

Khanal S., Kc K., Fulton J.P., Shearer S., Ozkan E. 2020. Remote sensing in agriculture - accomplishments, limitations, and opportunities. Remote Sens. 12:3783.

Kokkotos E., Zotos A., Patakas A. 2020. Evaluation of water stress coefficient Ks in different olive orchards. Agronomy 10:1594.

Langgut D., Cheddadi R., Carrión J.S., Cavanagh M., Colombaroli D., Eastwood W.J., Greenberg R., Litt T., Mercuri A.M., Miebach A. 2019. The origin and spread of olive cultivation in the Mediterranean Basin: The fossil pollen evidence. The Holocene 29:902-22.

Latham M. 1982. French soil classifications and their application in the South Pacific Islands. Available from: https://horizon.documentation.ird.fr/exl-doc/pleins_textes/pleins_textes_7/b_fdi_55-56/010022095.pdf

Latos B., Sobczak-Szelc K., Skocki K., Kozłowski R., Szczucińska A. 2018. Chemical composition of utility water in the arid climate zone on the examples of Kébili and Medenine regions (southern Tunisia). Pr. Geogr.:139-56.

Louis J., Debaecker V., Pflug B., Main-Knorn M., Bieniarz J., Mueller-Wilm U., Cadau E., Gascon F. 2016. Sentinel-2 Sen2Cor: L2A processor for users. pp. 1-8 in Proceedings Living Planet Symposium 2016, Spacebooks Online.

Magdich S., Ben Ahmed C., Boukhris M., Ben Rouina B., and Ammar E. 2015. Olive mill wastewater spreading effects on productivity and oil quality of adult chemlali olive (Olea europaea L.) in the South of Tunisia. Int. J. Agron. Agric. Res. 6:56-67.

Mimeau L., Tramblay Y., Brocca L., Massari C., Camici S., Finaud-Guyot P. 2021. Modeling the response of soil moisture to climate variability in the Mediterranean region. Hydrol. Earth Syst. Sci. 25:653-69.

Moreno R., Arias E., Sánchez J.L., Cazorla D., Garrido J., Gonzalez-Piqueras J. 2017. HidroMORE 2: An optimized and parallel version of HidroMORE. pp. 1-6 in 2017 8th International Conference on Information and Communication Systems (ICICS), IEEE.

Moriondo M., Leolini L., Brilli L., Dibari C., Tognetti R., Giovannelli A., Rapi B., Battista P., Caruso G., Gucci R. 2019. A simple model simulating development and growth of an olive grove. Eur. J. Agron. 105:129-45.

Mraidi I., El Asmi A.M., Skanji A. 2018. Conductivity and temperature corrections in the Djeffara Basin (Tunisia): impact of the basin heat flow reconstructions. pp. 97-100 in Conference of the Arabian Journal of Geosciences, Springer, The Netherlands.

Mtimet A. 2001. Soils of Tunisia. Options Mèdit. Sér. B 34:243-68.

Myhre B.E., Shih S.F. 1990. Using infrared thermometry to estimate soil water content for a sandy soil. Trans. ASAE 33:1-1486.

Nagaz K., Masmoudi M.M., Mechlia N.B. 2012. Impacts of irrigation regimes with saline water on carrot productivity and soil salinity. J. Saudi Soc. Agric. Sci. 11:19-27.

Napoli M., Orlandini S. 2015. Evaluating the Arc-SWAT2009 in predicting runoff, sediment, and nutrient yields from a vineyard and an olive orchard in Central Italy. Agric. Water Manag. 153:51-62.

Nasr J. Ben, Chaar H., Bouchiba F., Zaibet L. 2021. Assessing and building climate change resilience of farming systems in Tunisian semi-arid areas. Environ. Sci. Pollut. Res. 28:46797-808.

Neitsch S.L., Arnold J.G., Kiniry J.R., Williams J.R. 2011. Soil and water assessment tool theoretical documentation version 2009. Texas Water Resources Institute.

Nguyen H.-P., Bich T.N. 2019. Root system of olive trees (Olea Europaed L.) based on runoff harvesting system during dry period. Preprints 2019, 2019110016.

ODS 2019. Le Gouvernorat de Médenine en chiffres. Ministère du développement et de la coopération internationale, Tunis. Available from: http://www.ods.nat.tn/fr/index.php?id=32

Ortega-Salazar S., Ortega-Farías S., Kilic A., Allen R. 2021.

Performance of the METRIC model for mapping energy balance components and actual evapotranspiration over a superintensive drip-irrigated olive orchard. Agric. Water Manag. 251:106861.

Ortega T., Garrido J., Calera A., Marcuello C. 2019. Volumetric control for contrasting remote-sensing, in support of hydrological planning in Spain. pp. 117-130 in International Commission on Irrigation and Drainage (ICID)(Ed.), 3rd World Irrigation Forum. Development for Water, Food and Nutrition Security in a Competitive Environment.

Ouessar M. 2017. Climate change vulnerability of olive oil groves in dry areas of Tunisia: case study in the governorate of Médenine. pp. 41-52 in Rethinking Resilience, Adaptation and Transformation in a Time of Change. Springer, The Netherlands.

Ouessar M., Bruggeman A., Abdelli F., Mohtar R.H., Gabriels D., Cornelis W.M. 2009. Modelling water-harvesting systems in the arid south of Tunisia using SWAT. Hydrol. Earth Syst. Sci. 13:2003-21.

Ouessar M., Sghaier M., Fetoui M. 2008. Traditional and contemporary water harvesting techniques in the arid regions of Tunisia. What Makes Tradit. Technol. Tick? A Rev. Tradit. Approaches Water Manag. Drylands: 44.

Ouessar M., Yahyaoui H., Ouled Belgacem A., Boufalgha M. 2006. Aménagements et techniques de lutte contre la désertifcation: inventaire et bilan. In: Genin, D., Guillaume, H., Ouessar, M., Ouled Belgacem, A., Romagny, B., Sghaier, M., Taamallah H. (Eds.), Entre la désertification le développement la Jeffara tunisienne. CERES Ed. Tunis, Tunis. pp. 147-161. [In French].

Peel M.C., Finlayson B.L., McMahon T.A. 2007. Updated world map of the Köppen-Geiger climate classification. Hydrol. Earth Syst. Sci. 11:1633-44.

Piras F., Zanzana A., Costa Pinto L.M., Fiore B., Venturi M. 2021. The role of the jessour system for agrobiodiversity preservation in Southern Tunisia. Biodivers. Conserv. 1-16. [Epub ahead of print].

Raes D., Steduto P., Hsiao T.C., Fereres E. 2009. AquaCrop - the FAO crop model to simulate yield response to water: II. Main algorithms and software description. Agron. J. 101:438-47.

Rouina B.B., Trigui A., d'Andria R., Boukhris M., Chaieb M. 2007. Effects of water stress and soil type on photosynthesis, leaf water potential and yield of olive trees (Olea europaea L. cv. Chemlali Sfax). Aust. J. Exp. Agric. 47:1484-90.

Saadi S., Boulet G., Bahir M., Brut A., Delogu É., Fanise P., Mougenot B., Simonneaux V., Lili Chabaane Z. 2018. Assessment of actual evapotranspiration over a semiarid heterogeneous land surface by means of coupled low-resolution remote sensing data with an energy balance model: comparison to extra-large aperture scintillometer measurements. Hydrol. Earth Syst. Sci. 22:2187-209.

Saadi S., Simonneaux V., Boulet G., Raimbault B., Mougenot B., Fanise P., Ayari H., Lili-Chabaane Z. 2015. Monitoring irrigation consumption using high resolution NDVI image time series: Calibration and validation in the Kairouan Plain (Tunisia). Remote Sens. 7:13005-28.

Sánchez N., Martínez-Fernández J., Calera A., Torres E., Pérez-Gutiérrez C. 2010. Combining remote sensing and in situ soil moisture data for the application and validation of a distributed water balance model (HIDROMORE). Agric. Water Manag. 98:69-78.

Santos C., Lorite I.J., Allen R.G., Tasumi M. 2012. Aerodynamic parameterization of the satellite-based energy balance (METRIC) model for ET estimation in rainfed olive orchards of Andalusia, Spain. Water Resour. Manag. 26:3267-83.

Santos F. 2018. Assessing olive evapotranspiration partitioning from soil water balance and radiometric soil and canopy temperatures. Agronomy 8:43.

Saxton K.E., Rawls W. 2005. Soil water characteristics hydraulic properties calculator. Soil Sci. Soc. Am. J. 70:1569-78

Saxton K.E., Rawls W.J. 2006. Soil water characteristic estimates by texture and organic matter for hydrologic solutions. Soil Sci. Soc. Am. J. 70:1569-78.

Saxton K.E., Rawls W., Romberger J.S., Papendick R.I. 1986. Estimating generalized soil□water characteristics from texture. Soil Sci. Soc. Am. J. 50:1031-6.

Sbitri M.O., Serafini F. 2007. Production techniques in olive growing. International Olive Council, pp. 93-8. Available from: https://www.internationaloliveoil.org/wp-content/uploads/2019/12/Olivicultura_eng.pdf

Schiettecatte W., Ouessar M., Gabriels D., Tanghe S., Heirman S., Abdelli F. 2005. Impact of water harvesting techniques on soil and water conservation: a case study on a micro catchment in southeastern Tunisia. J. Arid Environ. 61:297-313.

Senkondo W., Munishi S.E., Tumbo M., Nobert J., Lyon S.W. 2019. Comparing remotely-sensed surface energy balance evapotranspiration estimates in heterogeneous and data-limited regions: A case study of Tanzania's Kilombero Valley. Remote Sens. 11:1289.

Sghaier M., Ouessar M., Belgacem A.O., Taamallah H., Khatteli H. 2010. Vulnerability of olive production sector to climate change in the governorate of Médenine (Tunisia). Final report. CI GRASP Proj.

Sheets K.R., Hendrickx J.M.H. 1995. Noninvasive soil water content measurement using electromagnetic induction. Water Resour. Res. 31:2401-9.

Soula R., Chebil A., McCann L., Majdoub R. 2021. Water scarcity in the Mahdia region of Tunisia: Are improved water policies needed? Groundw. Sustain. Dev. 12:100510.

Spyropoulos N.V, Dalezios N.R., Kaltsis I., Faraslis I.N. 2020. Very high resolution satellite-based monitoring of crop (olive trees) evapotranspiration in precision agriculture. Int. J. Sustain. Agric. Manag. Inf. 6:22-42.

Taamallah H. 2003. Carte pédologique de la Jeffara. Rapp. interne.[Soil Map Jeffara. Intern. report]. Jeffara Proj. IRA/IRD.

Tognetti R., d'Andria R., Morelli G., Alvino A. 2005. The effect of deficit irrigation on seasonal variations of plant water use in Olea europaea L. Plant Soil 273:139-55.

Torres P., Enrique A. 2010. El modelo FAO-56 asistido por satélite en la estimación de la evapotranspiración en un cultivo baja estrés hídrico y suelo desnudo. Available from: https://ruidera.uclm.es/xmlui/handle/10578/2811

Vogel J., Paton E., Aich V., Bronstert A. 2021. Increasing compound warm spells and droughts in the Mediterranean Basin. Weather Clim. Extrem. 32:100312.

Vossen P. 2007. Olive oil: history, production, and characteristics of the world's classic oils. HortSci. 42:1093-100.

Wagle P., Bhattarai N., Gowda P.H., Kakani V.G. 2017. Performance of five surface energy balance models for estimating daily evapotranspiration in high biomass sorghum. ISPRS J. Photogramm. Remote Sens. 128:192-203.

Wagner W., Naeimi V., Scipal K., de Jeu R., Martínez-Fernández J. 2007. Soil moisture from operational meteorological satellites. Hydrogeol. J. 15:121-31.

Yinglan A., Wang G., Liu T., Xue B., Kuczera G. 2019. Spatial

variation of correlations between vertical soil water and evapotranspiration and their controlling factors in a semi-arid region. J. Hydrol. 574:53-63.

Yves T., Koutroulis A., Samaniego L., Vicente-Serrano S.M., Volaire F., Boone A., Le Page M., Llasat M.C., Albergel C., Burak S. 2020. Challenges for drought assessment in the Mediterranean region under future climate scenarios. Earth-Science Rev.:103348. [Epub Ahead of Print]

Zeleke K.T. 2014. Water use and root zone water dynamics of drip-irrigated olive (Olea europaea L.) under different soil water regimes. N. Zeal. J. Crop Hortic. Sci. 42:217-32.

Zhang H., Han M., Chávez J.L., Lan Y. 2017. Improvement in estimation of soil water deficit by integrating airborne imagery data into a soil water balance model. Int. J. Agric. Biol. Eng. 10:37-46.

Zhang K., Kimball J.S., Running S.W. 2016. A review of remote sensing based actual evapotranspiration estimation. Wiley Interdiscip. Rev. Water 3:834-53.